THE JOURNAL OF PHYSICAL CHEMISTRY C
A JOURNAL OF THE AMERICAN CHEMICAL SOCIETY

pubs.acs.org/JPCC

Article

Temperature Dependence of Surface Band Bending in Layered BiTeI Semiconductor

Huacai Yan,[▽] Dandan Shi,[▽] Jingwei Dong,* Tianji Ou, Zhanfeng Liu, Yi Liu, Zhe Sun, and Zhongwei Chen*

Cite This: *J. Phys. Chem. C* 2025, 129, 9051−9056

Read Online

ACCESS | Metrics & More | Article Recommendations

ABSTRACT: The band bending effect at the surfaces of layered semiconducting materials is crucial for the overall performance of thermoelectric devices. However, a study dedicated to investigating the temperature dependence of the band bending effect in layered semiconductors has yet to be reported. The BiTeI semiconductor is a representative layered thermoelectric material, and this study directly investigated its electronic band structure as a function of temperature by utilizing photon-energy-dependent angle-resolved photoemission spectroscopy. The surface terminations of the crystal that we used were found to consist mainly of tellurium atoms. Additionally, the binding energies of the surface band increased by approximately 40 meV as the temperature rose from 10 to 100 K, which can be ascribed to the suppression of the electron transport process from the BiTeI surface to its bulk by phonon and defect. Our findings clearly provide direct evidence of temperature-dependent band bending in BiTeI.

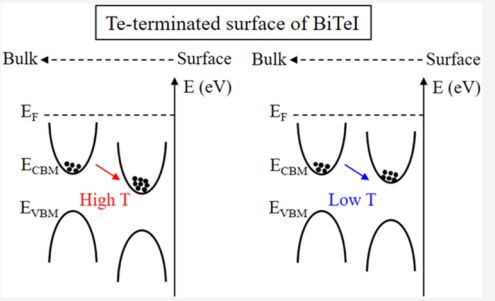

1. INTRODUCTION

Bismuth telluride iodide (BiTeI) is a fascinating material that falls under the category of semiconductor compounds.[1,2] It is part of the family of bismuth-based semiconductors, known for their unique thermoelectric properties, which allow them to efficiently convert temperature differences into electrical voltage and vice versa.[3−5] A comprehensive understanding of the electronic band structure is crucial to improving its performance in practical applications. The layered structure has been shown to exhibit a giant Rashba spin-splitting effect for conduction and valence bands both at the surface and in its bulk.[6,7] It also shows that the surface termination (I-terminated and Te-terminated atomic layers) significantly influences the n-type or p-type band structure at the surface.[8,9] Besides, the Rashba-split bands, as well as the band gap of BiTeI are quite sensitive to external parameters such as temperature and pressure.[10−12] The rich physical properties arise either from its intrinsic crystal structure or from specific extrinsic factors.

Band bending in semiconductors refers to the phenomenon where the energy bands of a semiconductor material curve or bend at the surface or interface. This effect is crucial for understanding various semiconductor properties and device behaviors, particularly in junctions, interfaces, and thin films. Although the prominent band bending in BiTeI has been studied extensively using angle-resolved photoemission spectroscopy (ARPES), scanning tunneling microscopy (STM), and density functional theory (DFT),[8,9] a detailed investigation of the relationship between band bending and the sample depth in real space has not been reported so far. Furthermore, as a thermoelectric material, a non-negligible band bending renormalization was also expected in BiTeI with certain variations in temperature, similar to a few other semiconductors such as boron-doped diamond and diamond-like films and GaAs.[13,14] A deeper understanding of these relationships can help bridge the gap between studies in the laboratory and practical applications of BiTeI at various sample depths and temperatures.

In this work, the effects of sample depth and temperature on the band bending near the surface of BiTeI were investigated using photon-energy-dependent ARPES. By monitoring the conduction and valence band structures at the surface, we revealed that the surface termination we used are tellurium atoms. Moreover, the band bending was found to be in the downward direction in the energy space with an increase of temperature, which indicates fewer electrons flow from the surface toward the bulk. This finding can be ascribed to the enhanced electron−phonon interaction and the redistribution of the defect concentration in the top layer and the sublayer. Our study not only sheds light on the temperature behavior of

Received: March 27, 2025
Revised: April 27, 2025
Accepted: April 29, 2025
Published: May 6, 2025

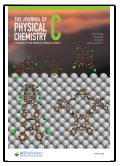

https://doi.org/10.1021/acs.jpcc.5c02036
J. Phys. Chem. C 2025, 129, 9051−9056

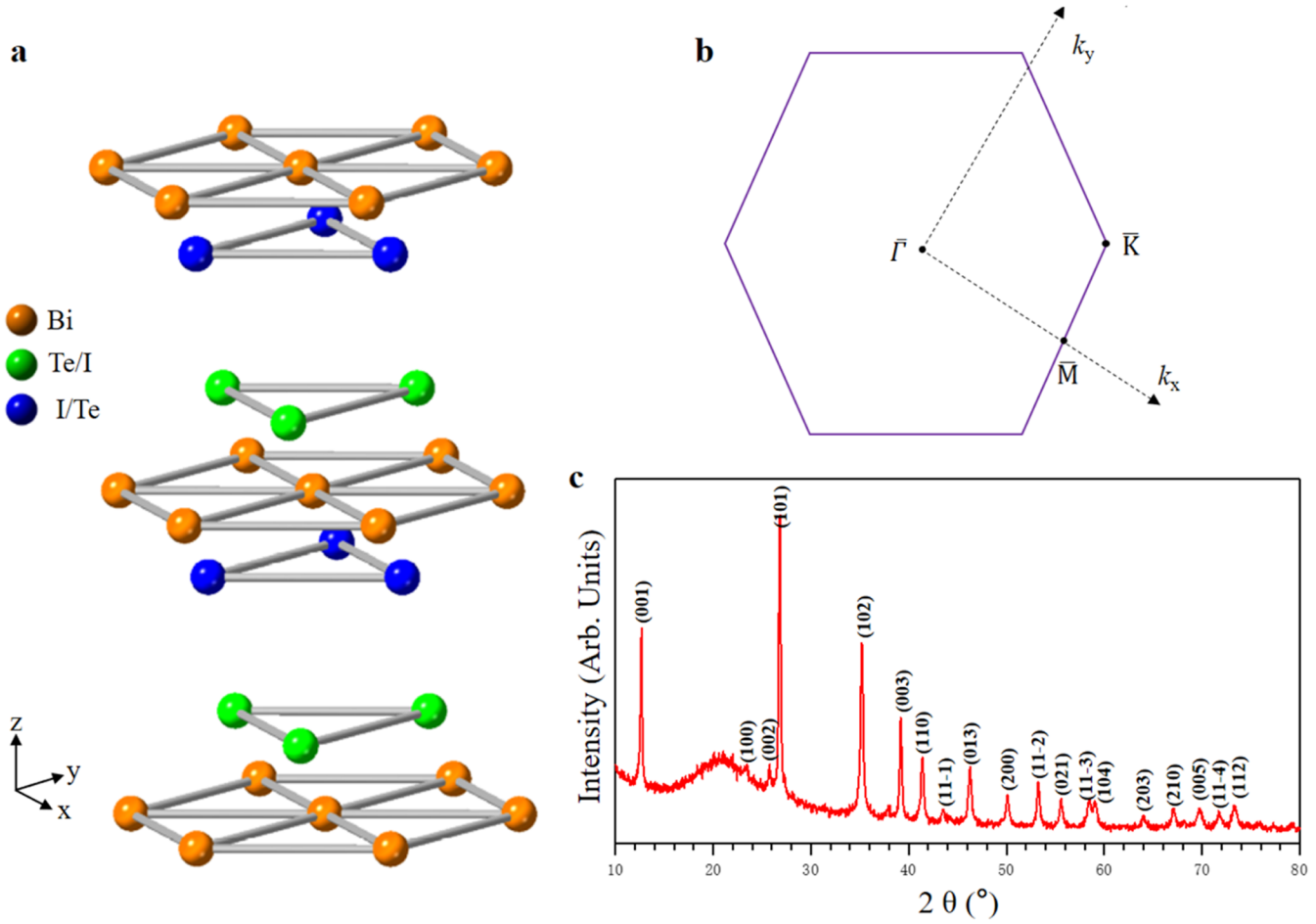

Figure 1. (a) Layered trigonal crystal structure of BiTeI. Schematic illustration of the two possible layer stacking orders along the *z*-axis. (b) Schematic diagram for the surface Brillouin zone of BiTeI. (c) XRD pattern of the BiTeI powder.

the surface band bending but also paves the way for versatile energy band engineering of the BiTeI semiconductor by a temperature knob.

2. EXPERIMENTAL DETAILS

The temperature-dependent ARPES data was collected at the BL13U beamline of the National Synchrotron Radiation Laboratory (NSRL) in Hefei, China. The energy and momentum resolutions of the hemispherical analyzer were better than 15 meV and 0.2°, respectively. The beam spot size at the sample position (horizontal × vertical) was approximately 0.3 mm × 0.3 mm. High-quality single crystals of BiTeI purchased from "Nanjing MKNANO Tech. Co., Ltd. (www.mukenano.com)" were cleaved at a temperature of 10 K and measured at a base pressure of lower than 7×10^{-11} Torr. The samples were characterized by using powder X-ray diffraction (XRD). Data collection at each photon energy and temperature was limited to under 10 min to minimize the aging effect of BiTeI.[15]

3. RESULTS AND DISCUSSION

Noncentrosymmetric layered BiTeI can exhibit two distinct layer stacking orders along the *z*-axis, terminating with either an iodine(I) layer or a tellurium (Te) layer, as shown in Figure 1(a). The covalent bonding between the Bi and Te planes forms a positively charged $(BiTe)^+$ bilayer. The weak coupling between the bilayer and the adjacent I plane provides a natural cleavage plane. Both "pure" and "mixed" terminations of the same crystal are randomly exposed by repeated cleaving due to the presence of stacking faults.[16] Typically, the morphology of the step edges at the mixed surface termination does not affect one another. It is important to note that the two terminations exhibit band bending in opposite directions owing to the surface charges.[8,9] The hexagonal-shaped surface Brillouin zone (SBZ) for BiTeI is shown in Figure 1(b). The powder XRD patterns of the BiTeI (refer to Figure 1(c)) match quite well with the standard JCPDS card No. 43−0650 (not shown), which represents the high purity of the crystals.

The Fermi surface of the BiTeI crystal acquired by 22 eV at 10 K is shown in Figure 2(a). The highly surface-sensitive ultraviolet (UV) light ARPES primarily provides photoemission maps from the near-surface region rather than the bulk of samples.[7,17] The surface band structures become more evident by the ARPES measurements with the energy range of 16−23 eV. The corresponding electronic states of BiTeI are shown in Figure 2(b). The bulk band is more distinct at 16 eV compared to higher photon energy values, while the surface band is more pronounced at 22 and 23 eV than at other energies. The surface conduction band dispersion from the Te atoms and the valence band dispersion from the I atoms. The more evident surface conduction band structure acquired at 18 and 22 eV, which indicates that the surface termination is Te atoms in our BeTeI samples. The surface domains generally exhibit a characteristic length scale of around 100 nm.[15] Thus,

https://doi.org/10.1021/acs.jpcc.5c02036
J. Phys. Chem. C 2025, 129, 9051−9056

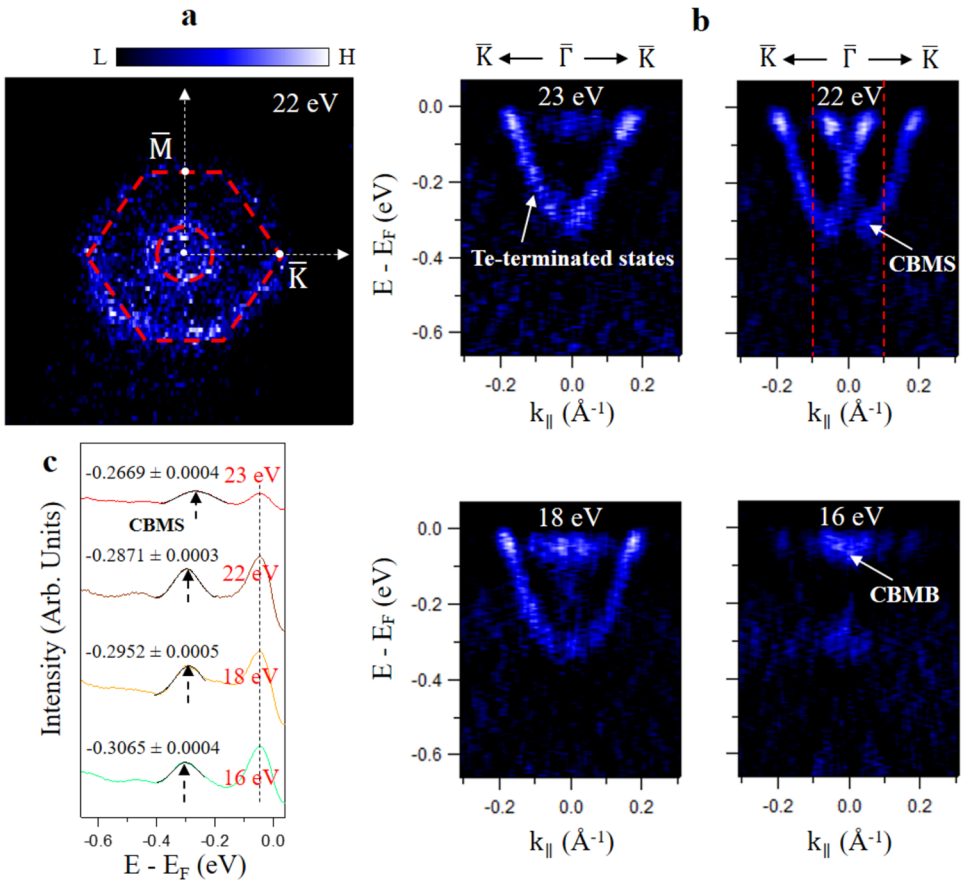

Figure 2. (a) Fermi surface of the BiTeI single crystal with Te termination acquired at a photon energy of 22 eV. (b) High-resolution ARPES maps of the BiTeI surface along the $\bar{\Gamma}$–$\bar{K}$ high-symmetry direction in the photon energy range 16–23 eV at 10 K. CBMS and CBMB represent the surface and bulk conduction band minimums, respectively. The Fermi level E_F in this work represents the chemical potential in the low-temperature limit (zero of the energy axis). (c) Energy distribution curves (EDCs) acquired (b) within a wavevector range of −0.1 to 0.1 Å^{-1} and centered at the $\bar{\Gamma}$ point. The black curves are Gaussian fits of the EDCs of the surface conduction band. The black dotted line indicates the peak position of the bulk states.

the UV light source with a beam spot size of 0.3 mm × 0.3 mm is capable of reflecting the real band structure of the surface atomic layers in BiTeI.

The energy distribution curves (EDCs) were obtained from the ARPES maps within a wavevector range of −0.1 to 0.1 (Å^{-1}) centered at $\bar{\Gamma}$ using various photon energies (Figure 2(c)). These curves were used to investigate the band bending effect at various sample depths. The binding energy of CBMS is roughly 0.2669 eV using 23 eV photon energy, and the value is 0.3065 eV using the photon energy of 16 eV. The CBMS downshift toward the higher binding energy level was observed as the photon energy increased from 23 to 16 eV. This implies that the surface exhibits a p-type band bending similar to the result obtained for the Te-terminated BiTeI. This is in agreement with a previous study conducted using the two different photon energies of 21.2 and 6.994 eV.[6] Different photon energies correspond to the different photoelectron detection depths in the BiTeI crystal.[17] It should be stressed here that the probing depth of the photon energy of 23 eV (0.4–0.7 nm) is much smaller compared to the typical length for surface band bending. The thicknesses of the depletion and accumulation layers are estimated to be about 3 nm.[9]

Temperature is an effective parameter for tuning the band gaps of semiconductors.[18−20] It has been shown that the band gap of BiTeI can be renormalized by varying the temperature as well.[21] The ARPES map by the photon energies of 16 eV at 100 K is shown in Figure 3(a). The extracted energy distribution curves from Figures 2(b) and 3(a) are presented in Figure 3(b), which exhibits an evident CBMS downshift of approximately 30 meV upon heating. Figure 3(c,d) shows the ARPES maps at 10 and 100 K by 21 eV, respectively. Similarly, the corresponding energy distribution curves show a CBMS downshift of approximately 30 meV while the CBMB remains stable with the increase from 10 to 100 K at 21 eV (Figure 3(e)). The surface band structure shows a clear evolution upon heating even if using various photon energies. The band downshift can be ascribed to a reduction in the electron density from the surface states to the bulk states of BiTeI. The energy resolution of the analyzer is better than 15 meV, the value from the photon beam is close to 2 meV, and the thermalization contribution of the temperature difference of roughly 100 K to the energy resolution is approximately 9 meV; thus, the overall energy resolution of the heating experiment is roughly 18 meV that is lower the band-downshift value.

In view of the above external factors, the predominant factor of the temperature-dependent band shift should be others. A higher surface electron density corresponded to a larger surface band bending.[13,15] The antisite I_{Te} and Te_I are the most commonly found defects in BiTeI owing to the similar atomic radii of Te^{2-} (2.07 Å) and I^- (2.06 Å).[22,23] The high concentration of defects leads to high electron scattering and

https://doi.org/10.1021/acs.jpcc.5c02036
J. Phys. Chem. C 2025, 129, 9051−9056

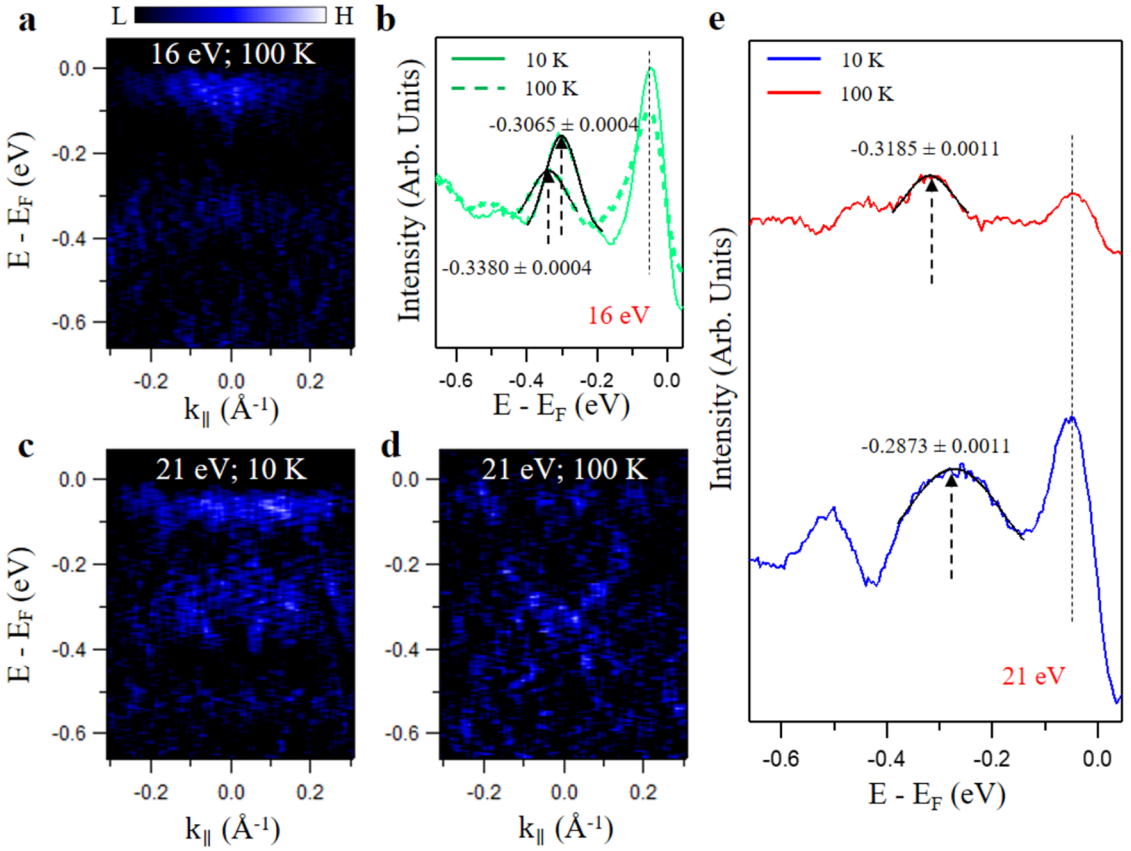

Figure 3. (a) ARPES maps of BiTeI with Te termination along the $\bar{\Gamma}-\bar{K}$ high-symmetry direction with photon energies of 16 eV at 100 K. (b) Energy distribution curves extracted from the ARPES band maps in (a) within a wavevector range of 0−0.2 ($Å^{-1}$) centered at $\bar{\Gamma}$. The corresponding energy distribution curves at a temperature of 10 K from Figure 2 (b) are shown as well. (c, d) ARPES maps along the $\bar{\Gamma}-\bar{K}$ high-symmetry direction at 10 and 100 K by 21 eV, respectively. (d) Energy distribution curves extracted from the maps in (c, d). The black dotted line indicates the peak position of the bulk states.

reduced carrier mobility.[15,24] There was a negligible change in the total carrier concentration, while the carrier mobility apparently reduced as the temperature was raised beyond a temperature of 100 K for the BiTeI crystal. This could be attributed to the increasing influence of the acoustical phonons combined with the change in density of the I_{Te} and Te_I defects at the top layer and the sublayer as described by a study undertaken by Wu et al.[25] In addition, as shown in Figure 4, we observed different core-level shifts. For example, the Bi 5d orbital exhibited a 0.3 eV difference between 300 and 100 K, while the Te 4d and I 4d orbitals showed a 0.5 eV difference between these temperatures. These different shifts correspond to different kinetic energies, which are associated with varying detection depths.

A schematic diagram depicting the primary mechanism behind the band bending at the Te surface of the BiTeI samples due to an increase in temperature is presented in Figure 5. The electrons gather on the sample surface and cannot flow into the bulk phase upon heating, which induces the downward band bending. This study clearly suggested that the variable acoustical phonon number and defect density between the top layer and the sublayer had a huge impact on the electron transport mechanism from the surface of BiTeI to its bulk.

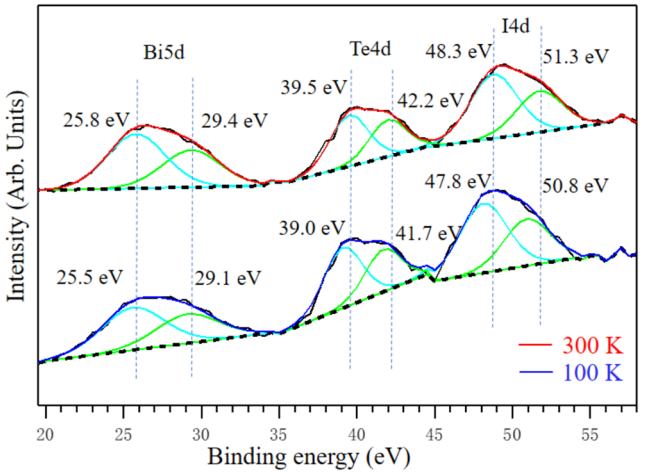

Figure 4. High-resolution XPS of the BiTeI single crystal with Te termination obtained at 300 and 100 K (hv = 1254 eV). Cyan and green curves represent the $d_{5/2}$ and $d_{3/2}$ of Bi 5d, Te 4d, and I 4d fit results at 300 and 100 K, respectively. The blue dotted lines indicate the peak positions of the $d_{5/2}$ and $d_{3/2}$ at 300 K.

4. CONCLUSIONS

In conclusion, the electronic band structure of BiTeI was measured at different temperatures using photon-energy-dependent ARPES. An energy comparison of the surface band at various photoelectron escape depths reveals that its

https://doi.org/10.1021/acs.jpcc.5c02036
J. Phys. Chem. C 2025, 129, 9051−9056

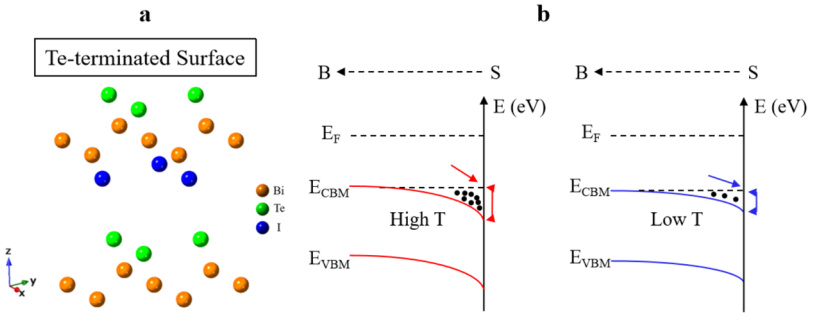

Figure 5. Schematic diagram depicting the surface band bending for the Te surface-terminated BiTeI. *B* and *S* represent the bulk and surface of BiTeI, respectively.

surface atomic termination is that of tellurium atoms. In addition, the downward band bending was observed with an increase in the crystal temperature. This study provides sufficient evidence to suggest that the electron transport process from the surface states to the bulk states of BiTeI is suppressed by the increased phonon density and the redistribution of defect concentration at the top layer and the sublayer upon heating. Our study establishes a foundation for connecting laboratory research with practical applications of layered BiTeI.

AUTHOR INFORMATION

Corresponding Authors

Jingwei Dong − *Power Battery & Systems Research Center and State Key Laboratory of Catalysis, Dalian Institute of Chemical Physics, Chinese Academy of Sciences, Dalian 116023, China*; Email: djw1991@dicp.ac.cn

Zhongwei Chen − *Power Battery & Systems Research Center and State Key Laboratory of Catalysis, Dalian Institute of Chemical Physics, Chinese Academy of Sciences, Dalian 116023, China*; orcid.org/0000-0003-3463-5509; Email: zwchen@dicp.ac.cn

Authors

Huacai Yan − *School of Materials Science and Engineering, Peking University, Beijing 100871, China*; orcid.org/0000-0003-3957-3925

Dandan Shi − *Jilin Engineering Normal University, Changchun 130052, China*

Tianji Ou − *Research Team of Extreme Condition Physics, College of Physics and Electronic Information, Inner Mongolia Minzu University, Tongliao 028000, China*

Zhanfeng Liu − *National Synchrotron Radiation Laboratory, University of Science and Technology of China, Hefei 230029, China*

Yi Liu − *National Synchrotron Radiation Laboratory, University of Science and Technology of China, Hefei 230029, China*

Zhe Sun − *National Synchrotron Radiation Laboratory, University of Science and Technology of China, Hefei 230029, China*

Complete contact information is available at: https://pubs.acs.org/10.1021/acs.jpcc.5c02036

Author Contributions

[▽]H.Y. and D.S. contributed equally to this work.

Notes

The authors declare no competing financial interest.

ACKNOWLEDGMENTS

This work was supported by the National Natural Science Foundation of China (Grant Nos. 12104245, 22409194), the Energy Revolution S&T Program of Yulin Innovation Institute of Clean Energy, (Grant No. YlCE E411060316), and the Strategic Priority Research Program of the Chinese Academy of Sciences (Grant Nos. XDB0600000, XDB0600200).

REFERENCES

(1) Bahramy, M. S.; Arita, R.; Nagaosa, N. Origin of giant bulk Rashba splitting: Application to BiTeI. *Phys. Rev. B* **2011**, *84* (4), No. 041202.

(2) Bianca, G.; Trovatello, C.; Zilli, A.; Zappia, M. I.; Bellani, S.; Curreli, N.; Conticello, I.; Buha, J.; Piccinni, M.; Ghini, M.; et al. Liquid-Phase Exfoliation of Bismuth Telluride Iodide (BiTeI): Structural and Optical Properties of Single-/Few-Layer Flakes. *ACS Appl. Mater. Interfaces* **2022**, *14* (30), 34963−34974.

(3) Kulbachinskii, V. A.; Kytin, V. G.; Lavrukhina, Z. V.; Kuznetsov, A. N.; Markelov, A. V.; Shevelkov, A. V. Thermoelectric Properties of BiTeI with Addition of BiI_3, CuI, and Overstoichiometric Bi. *Semiconductors* **2011**, *45* (7), 845−849.

(4) Kulbachinskii, V. A.; Kytin, V. G.; Kudryashov, A. A.; Kuznetsov, A. N.; Shevelkov, A. V. On the electronic structure and thermoelectric properties of BiTeBr and BiTeI single crystals and of BiTeI with the addition of BiI_3 and CuI. *J. Solid State Chem.* **2012**, *193*, 154−160.

(5) Ideue, T.; Ye, L.; Checkelsky, J. G.; Murakawa, H.; Kaneko, Y.; Tokura, Y. Thermoelectric probe for Fermi surface topology in the three-dimensional Rashba semiconductor BiTeI. *Phys. Rev. B* **2015**, *92* (11), No. 115114.

(6) Ishizaka, K.; Bahramy, M. S.; Murakawa, H.; Sakano, M.; Shimojima, T.; Sonobe, T.; Koizumi, K.; Shin, S.; Miyahara, H.; Kimura, A.; et al. Giant Rashba-type spin splitting in bulk BiTeI. *Nat. Mater.* **2011**, *10* (7), 521−526.

(7) Landolt, G.; Eremeev, S. V.; Koroteev, Y. M.; Slomski, B.; Muff, S.; Neupert, T.; Kobayashi, M.; Strocov, V. N.; Schmitt, T.; Aliev, Z. S.; et al. Disentanglement of Surface and Bulk Rashba Spin Splittings in Noncentrosymmetric BiTeI. *Phys. Rev. Lett.* **2012**, *109* (11), No. 116403.

(8) Crepaldi, A.; Moreschini, L.; Autes, G.; Tournier-Colletta, C.; Moser, S.; Virk, N.; Berger, H.; Bugnon, P.; Chang, Y. J.; Kern, K.; et al. Giant Ambipolar Rashba Effect in the Semiconductor BiTeI. *Phys. Rev. Lett.* **2012**, *109* (9), No. 096803.

(9) Butler, C. J.; Yang, H.-H.; Hong, J.-Y.; Hsu, S.-H.; Sankar, R.; Lu, C.-I.; Lu, H.-Y.; Yang, K.-H. O.; Shiu, H.-W.; Chen, C.-H.; et al. Mapping polarization induced surface band bending on the Rashba semiconductor BiTeI. *Nat. Commun.* **2014**, *5* (1), No. 4066.

(10) Monserrat, B.; Vanderbilt, D. Temperature dependence of the bulk Rashba splitting in the bismuth tellurohalides. *Phys. Rev. Mater.* **2017**, *1* (5), No. 054201.

(11) Bahramy, M. S.; Yang, B. J.; Arita, R.; Nagaosa, N. Emergence of non-centrosymmetric topological insulating phase in BiTeI under pressure. *Nat. Commun.* **2012**, *3* (1), No. 679.

https://doi.org/10.1021/acs.jpcc.5c02036
J. Phys. Chem. C 2025, 129, 9051−9056

(12) Güler-Kılıç, S.; Kılıç, Ç. Pressure dependence of the band-gap energy in BiTeI. *Phys. Rev. B* **2016**, *94* (16), No. 165203.
(13) Chen, S. Y.; Lue, J. T. Temperature dependence of surface band bending and field emission for boron-doped diamond and diamond-like films. *New J. Phys.* **2002**, *4*, No. 79.
(14) Stiles, K.; Mao, D.; Kahn, A. Oxygen adsorbed on GaAs(110) surfaces: The effect of temperature on band bending. *J. Vac. Sci. Technol., B:Microelectron. Process. Phenom.* **1988**, *6* (4), 1170−1173.
(15) Fiedler, S.; El-Kareh, L.; Eremeev, S. V.; Tereshchenko, O. E.; Seibel, C.; Lutz, P.; Kokh, K. A.; Chulkov, E. V.; Kuznetsova, T. V.; Grebennikov, V. I.; et al. Defect and structural imperfection effects on the electronic properties of BiTeI surfaces. *New J. Phys.* **2014**, *16*, No. 075013.
(16) Tournier-Colletta, C.; Autes, G.; Kierren, B.; Bugnon, P.; Berger, H.; Fagot-Revurat, Y.; Yazyev, O. V.; Grioni, M.; Malterre, D. Atomic and electronic structure of a Rashba p−n junction at the BiTeI surface. *Phys. Rev. B* **2014**, *89* (8), No. 085402.
(17) Seah, M. P.; Dench, W. A. Quantitative electron spectroscopy of surfaces: A standard data base for electron inelastic mean free paths in solids. *Surf. Interface Anal.* **1979**, *1* (1), 2−11.
(18) Fan, H. Y. Temperature dependence of the energy gap in semiconductors. *Physica* **1951**, *82* (6), 900−905.
(19) Cardona, M.; Meyer, T. A.; Thewalt, M. L. W. Temperature dependence of the energy gap of semiconductors in the low-temperature limit. *Phys. Rev. Lett.* **2004**, *92* (19), No. 196403.
(20) Chen, C.; Chen, F.; Chen, X.; Deng, B.; Eng, B.; Jung, D.; Guo, Q.; Yuan, S.; Watanabe, K.; Taniguchi, T.; et al. Bright Mid-Infrared Photoluminescence from Thin-Film Black Phosphorus. *Nano Lett.* **2019**, *19* (3), 1488−1493.
(21) Brousseau-Couture, V.; Antonius, G.; Côté, M. Temperature dependence of the topological phase transition of BiTeI from first principles. *Phys. Rev. Res.* **2020**, *2* (2), No. 023185.
(22) Shannon, R. D. Revised effective ionic radii and systematic studies of interatomic distances in halides and chalcogenides. *Acta Crystallogr., Sect. A* **1976**, *32*, 751−767.
(23) Horák, J.; Tichy, L.; Lostak, P. Electrical conductivity of BiTeI crystals. *Phys. Status Solidi A* **1981**, *63* (2), 407−416.
(24) Li, Z.; Zhao, C.; Xiao, C. Defect Compensation Weakening Induced Mobility Enhancement in Thermoelectric BiTeI by Iodine Deficiency. *Chem. - Asian J.* **2020**, *15* (23), 4124−4129.
(25) Wu, L.; Yang, J.; Chi, M.; Wang, S.; Wei, P.; Zhang, W.; Chen, L.; Yang, J. Enhanced Thermoelectric Performance in Cu-Intercalated BiTeI by Compensation Weakening Induced Mobility Improvement. *Sci. Rep.* **2015**, *5* (1), No. 14319.

https://doi.org/10.1021/acs.jpcc.5c02036
J. Phys. Chem. C 2025, 129, 9051−9056